Available online at www.dergipark.org.tr/en

INTERNATIONAL ADVANCED RESEARCHES and ENGINEERING JOURNAL

Journal homepage: www.dergipark.org.tr/en/pub/iarej

e-ISSN: 2618-575X

International Open Access

Volume 05
Issue 02

August, 2021

Research Article

A numerical study of the natural convection of Al_2O_3-EG nanofluid in a square enclosure and impacts and a comparison of various viscosity and thermal conductivity models

Nese Keklikcioglu Cakmak [a,*], ***Hasan Hüseyin Durmazucar*** [a] ***and Kerim Yapici*** [b]

[a]*Department of Chemical Engineering, Faculty of Engineering, Sivas Cumhuriyet University, Sivas, Turkey,*
[b]*Department of Chemical Engineering, Faculty of Engineering, Süleyman Demirel University, Isparta, Turkey*

ARTICLE INFO

Article history:
Received 02 January 2021
Revised 15 May 2021
Accepted 09 June 2021

Keywords:
Al_2O_3
Finite volume method
Fourth-order linear scheme
Lid-driven cavity
Nanofluid
Natural convection
Thermal conductivity
Viscosity

ABSTRACT

In the current study, heat transfer enhancement in an enclosure was investigated by utilizing Al_2O_3-EG nanofluid. In the numerical solutions, the solid-liquid mixture equations were applied for the enclosure that composed alumina-ethylene glycol nanofluid, in terms of the two-dimensional buoyancy-driven convection. Various viscosity and thermal conductivity models were utilized for the purpose of assessing heat transfer improvement. The purpose of this study was to reveal the impacts caused by uncertainties in the viscosity and thermal conductivity of the nanofluid on laminar natural convection heat transfer occurring in a square enclosure. The temperatures of the right and left vertical walls of the enclosure were kept constant as Tc and Th, respectively, whereas the thermal insulation of the other walls was performed. The discretization of the governing equations was performed by utilizing the finite volume method and the SIMPLE algorithm. Calculations were made for the Rayleigh number (10^3-10^6) and the volume fraction of alumina nanoparticles, ϕ= 0-5%. In this study, many parameters affecting heat transfer by natural convection were investigated in the enclosure containing Al_2O_3-EG nanofluid, and it was found that nanofluid viscosity was the most efficient factor for heat transfer rate.

1. Introduction

Because of its broad range of applications in the cooling of nuclear reactors, chemical processes, micro/mini-channel heat sinks, automobiles, solar energy collections, electronic system components, and heat exchangers, natural convection heat transfer represents a significant phenomenon in engineering systems [1-7]. In such systems, heat transfer increase is important for energy and industrial conservation. The fact that the thermal conductivity of conventional heat transfer fluids, including oil, ethylene glycol (EG), and water is low is regarded to be the main restriction on improving the performance and compactness of such thermal systems. Researchers conduct comprehensive studies for the purpose of revealing novel ways to meet the industrial requirements in the field of these thermal systems. The idea of Maxwell to suspend micrometer or metallic millimeter-sized particles to be able to improve the thermal conductivity of fluids is broadly known [8]. Nevertheless, it is not possible to utilize these particles in micro-devices since they can lead to a number of significant issues, including the abrasion of the heat transfer device such as a pipeline, cooling channels, etc., blocking of the flow channels, and increasing in the pressure decrease in the fluid. Thus, fluids containing large suspended particles have limited practical applications in enhancing heat transfer. Nevertheless, modern nanotechnology presents significant opportunities for producing materials that have a mean size of 100 nanometer or below. The above-mentioned particles may disperse well in traditional working fluids for the purpose of generating a new heat transfer fluid type, which is known under the name of nanofluid [9]. There is a strong dependence of the management and

* Corresponding author. Tel.: +90-346-219-1010 / 2232 ; Fax: +90-346-219-1010.
E-mail addresses: nkeklikcioglu@cumhuriyet.edu.tr *(N. Keklikcioglu Cakmak)*, hdurmaz@cumhuriyet.edu.tr *(H.H. Durmazucar)*, kerimyapici@gmail.com *(K. Yapici)*
ORCID: 0000-0002-8634-9232 *(N. Keklikcioglu Cakmak)*, 0000-0003-2454-7003 *(H. H. Durmazucar)*, 0000-0002-3902-9375 *(K. Yapici)*
DOI: 10.35860/iarej.852562

miniaturization of engineering systems in thermal terms on the enhancement of working fluids' thermal behaviors. Comprehensive research has been conducted recently on a novel technique developed to enhance heat transfer by utilizing nano-scale particles that are dispersed in a base fluid, which is as also called nanofluid. Nanofluids, as new heat transfer fluids, may take a significant part in enhancing the thermal effectiveness of engineering devices, including cooling systems and heat exchangers. Comprehensive studies were carried out in the last ten years on convective heat transfer by utilizing nanofluids [10, 11]. Some researchers have carried out studies to improve the heat transfer-related properties of forced convection applications. On the contrary, not enough attention has been paid to enhancing heat transfer in applications regarding natural convection. As a first, Khanafer et al. [12] conducted a research on natural convection heat transfer inside a nanofluid-filled rectangular enclosure. A numerical natural convection simulation modeled as two-dimensional is presented for a nanofluid-filled vertical enclosure. The study showed that thanks to the volumetric fraction emerging in copper nanoparticles in the water at a specified Grashof number, an increase occurred in heat transfer through the enclosure. Hwang et al. [13] theoretically investigated the natural convection caused by the temperature change between the lower and upper walls and the adiabatic sidewalls in a rectangular cavity with water-Al_2O_3 nanofluids. They found that the increased nanoparticle size caused the deterioration of the natural rate of convection in the enclosure. Abu-Nada [14] investigated the impact of different characteristics of Al_2O_3–water nanofluids on natural convection in a circular medium. The researcher determined that for $Ra \geq 10^4$, the heat transfer increased as the concentration of nanoparticles increased. However, improvement occurred in heat transfer at $Ra = 10^3$. By using nanofluids for different related parameters, Oztop and Abu-Nada [15] studied the improvement of heat transfer in a rectangular enclosure. The researchers stated that the reason for the improvement of heat transfer was the increased heater size and the Rayleigh (Ra) number. Corcione et al. [16] conducted the analysis of heat transfer in an enclosure, which was filled with a nanofluid, and obtained the findings indicating that an increase in nanoparticle concentration caused an increase in the performance of the heat transfer. Furthermore, the scholars revealed that as the average nanofluid temperature and width of the enclosure increased and the size of the nanoparticle decreased, the heat transfer increased. Mahalakshmi et al. [17] carried out a quantitative research related to the natural convective heat transfer in an enclosure with a center heater by utilizing nanofluids. They showed that an increase occurred in heat transfer with the increased heater length in both horizontal and vertical positions for the increased Rayleigh numbers. Especially a more significant increase was observed in heat transfer due to a heater located in a vertical position of a maximum length. Yıldız et al. [18] conducted a comparative research to examine the thermal conductivity model on mono and hybrid nanofluids. A recently conducted numerical study demonstrated a lower thermal conductivity acquired by utilizing a number of theoretical and numerical models in comparison with their study because of ignoring a number of significant factors, such as nanoparticles' shapes and sizes.

Nevertheless, the results of experimental research related to the subject are contradictory [13, 19-21]. Accordingly, the dispersion of nanoparticles in a base fluid can lead to a considerable decrease, not the improvement, in the natural convection heat transfer in enclosures. Putra et al. [22] investigated the natural convection heat transfer of nanofluids experimentally in a horizontal cylinder. In their study, heating and cooling were performed from two ends, respectively. They found that with the use of CuO / water and Al_2O_3 / water nanofluids, the natural convective heat transfer undergoes a definite degradation depending on the cylinder's particle density, aspect ratio, and concentration. It was also found that with particle concentration, an increase occurred in the deterioration and it was more considerable in terms of CuO nanofluids. For instance, it was identified that at the 5×10^7 Rayleigh number, there were 150% and 300% reductions in the Nusselt number for 4 wt% of Al_2O_3 and CuO, respectively. Similar to Putra et al. [22], Wen and Ding [19] revealed a reduction in the coefficient of the natural convective heat transfer in comparison with pure water. Moreover, an increase was observed in the deterioration in question with nanoparticle concentration. For their observations, the researchers suggested a number of potential techniques, including the convection induced by a difference in concentration, interactions between particle-particle and particle-fluid, and modified dispersion characteristics.

For the mentioned difference among the numerical estimations and experimental findings with regard to the natural convection heat transfer efficiency of utilizing nanofluids in enclosures, the potential factors that ensures contribution can be vary in terms of the shape and size of particles, the distribution of particles, and uncertainty observed in the thermo-physical properties of nanofluids, particularly the effective dynamic viscosity and thermal conductivity. Therefore, the goal of this research is to investigate, through numerical simulations, the impacts of uncertainties because of employing various formulate in terms of the efficient thermal conductivity and dynamic viscosity of the Al_2O_3-EG nanofluid on the properties related to the natural convection heat transfer occurring in a vertical square enclosure. In addition, in a part of this study, an evaluation of thermophysical properties, such as

thermal conductivity and viscosity, obtained by using experimental data on heat transfer in natural convection are presented.

2. Problem Statement and Mathematical Formulation

Figure 1 presents the physical models discussed in this study, the related boundary conditions, and geometric dimensions. Figure 1 is utilized with the aim of examining the natural convection heat transfer. A square cavity having stationary walls is investigated. Temperatures of the right and left walls belonging to the cavity are kept steady as cold (TC) and hot (TH), respectively. On the other hand, the walls at the bottom and top are kept as adiabatic. In terms of a series of the Rayleigh numbers, the analysis of the flow and heat transfer phenomena was performed for the case of natural convection. In the case, Al_2O_3-EG nanofluid was considered.

The thermophysical characteristics of Al_2O_3 nanoparticles and EG are shown in Table 1.

Utilizing the Boussinesq approximation and ignoring the viscous dissipation impact, the mathematical model for natural convection was obtained. For the Cartesian coordinate in two dimensions, it is possible to write the dimensionless governing equations in the following way:

$$\frac{\partial u}{\partial x}+\frac{\partial v}{\partial y}=0 \tag{1}$$

$$u\frac{\partial u}{\partial x}+v\frac{\partial v}{\partial y}=-\frac{1}{\rho_{nf}}\frac{\partial p}{\partial x}+\nu_{nf}\left(\frac{\partial^2 u}{\partial x^2}+\frac{\partial^2 u}{\partial y^2}\right) \tag{2}$$

$$u\frac{\partial v}{\partial x}+v\frac{\partial v}{\partial y}=-\frac{1}{\rho_{nf}}\frac{\partial p}{\partial y}+\nu_{nf}\left(\frac{\partial^2 v}{\partial x^2}+\frac{\partial^2 v}{\partial y^2}\right)+g\beta_{nf}(T-T_c) \tag{3}$$

$$u\frac{\partial T}{\partial x}+v\frac{\partial T}{\partial y}=\alpha_{nf}\left(\frac{\partial^2 T}{\partial x^2}+\frac{\partial^2 T}{\partial y^2}\right) \tag{4}$$

The above-mentioned governing equations are obtained by utilizing the non-dimensional quantities presented below:

$$x'=\frac{x}{H},\quad y'=\frac{y}{H},\ u'=\frac{uH}{\alpha_f},\quad v'=\frac{vH}{\alpha_f},\quad p'=\frac{pH^2}{\rho_{nf}{\alpha_f}^2},\ \theta=\frac{T-T_C}{T_H-T_C} \tag{5}$$

where quantities shown with a prime mark refer to the dimensional forms of the primitive variables. In Equation 6, calculation of the dimensionless Prandtl (Pr) and Rayleigh (Ra) numbers are shown.

Figure 1 demonstrates the natural convection-related boundary conditions. It is seen that on every wall of the square cavity, the boundary condition of no-slip velocity is implemented. Regarding the non-dimensional temperature (θ), on the left wall (θ =1) and the right wall (θ =0), a constant boundary condition is set.

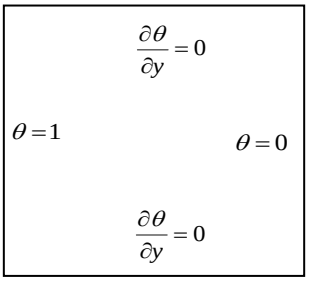

Figure 1. The natural convection problem

Table 1. Thermophysical characteristics of fluid (EG) and Al_2O_3 nanoparticles [23, 24]

	ρ	c_p	k	μ	β
	kgm^{-3}	$Jkg^{-1}K^{-1}$	$Wm^{-1}K^{-1}$	$kgm^{-1}s^{-1}$	K^{-1}
Al_2O_3	3970	765	40	-	$0.85x10^{-5}$
Ethylene Glycol	1114	2415	0.252	0.0161	$5.7x10^{-4}$

$$Ra=\frac{g\beta\Delta TH^3}{\nu\alpha}\qquad Pr=\frac{\nu}{\alpha} \tag{6}$$

While keeping the walls at the top and bottom as adiabatic, a zero-flux boundary condition is implemented. Furthermore, the solution of problems related to the natural convection is achieved by utilizing Al_2O_3-EG nanofluid as a working fluid. In order to solve Al_2O_3-EG nanofluid, the approach of homogeneous single-phase is employed, and thus, the Al_2O_3-EG nanofluid replaces the physical characteristics of the Newtonian fluid mentioned above. It is possible to write the non-dimensional governing equations in the way presented below:

$$\frac{\partial u'}{\partial x'}+\frac{\partial v'}{\partial y'}=0 \tag{7}$$

$$u'\frac{\partial u'}{\partial x'}+v'\frac{\partial v'}{\partial y'}=-\frac{\partial p'}{\partial x'}+\frac{\mu_{nf}}{\rho_{nf}\alpha_f}\left(\frac{\partial^2 u'}{\partial x'^2}+\frac{\partial^2 u'}{\partial y'^2}\right) \tag{8}$$

$$u'\frac{\partial v'}{\partial x'}+v'\frac{\partial v'}{\partial y'}=-\frac{\partial p'}{\partial y}+\frac{\mu_{nf}}{\rho_{nf}\alpha_f}\left(\frac{\partial^2 v'}{\partial x'^2}+\frac{\partial^2 v'}{\partial y'^2}\right)+\frac{\beta_{nf}}{\beta_f}Ra\,Pr\,\theta \tag{9}$$

$$u'\frac{\partial\theta}{\partial x'}+v'\frac{\partial\theta}{\partial y'}=\frac{\alpha_{nf}}{\alpha_f}\left(\frac{\partial^2\theta}{\partial x'^2}+\frac{\partial^2\theta}{\partial y'^2}\right) \tag{10}$$

In these equations, *nf* refers to the features of the Al_2O_3-EG nanofluid. On the other hand, *f* denotes the characteristics of

the base fluid (EG). The non-dimensional quantities given in Equations from 7 to 10 are described by utilizing base fluid characteristics and they are also presented in Equation 6.

The governing flow equations are discretized by using the finite volume method. The second-order central differencing scheme is utilized to approximate the diffusion terms in the governing equations. On the other hand, the non-uniform form of the four-point fourth-order interpolation scheme proposed by Yapici and Obut [25] is utilized to be able to approximate convective terms.

Various correlations related to the physical characteristics of the Al_2O_3-EG nanofluid are introduced in the literature. In the present research, 2 cases formed by combining 8 different viscosity and 2 different thermal conductivity correlation model equations presented in tables 2 and 3 were investigated. While the combination of 8 various viscosity models was formed with the thermal conductivity model proposed by Maxwell [8] in the first case, the combination of 8 various viscosity models with the thermal conductivity model proposed by Chandrasekar et al. [26] was formed in the second case.

Where ϕ denotes the volume fraction of Al_2O_3 nanoparticles in the base fluid (EG). By utilizing the mixing rule, the heat capacity (C_{pnf}), thermal expansion coefficient (β_{nf}), density (ρ_{nf}), and molecular weight (M_{nf}) of the Al_2O_3-EG nanofluid are assessed [26]:

$$\rho_{nf} = (1-\varphi)\rho_f + \varphi\rho_p \quad (11)$$

$$C_{p_{nf}} = \frac{(1-\varphi)Cp_f\rho_f + \varphi Cp_p\rho_p}{\rho_{nf}} \quad (12)$$

$$\beta_{nf} = \frac{(1-\varphi)\beta_f\rho_f + \varphi\beta_p\rho_p}{\rho_{nf}} \quad (13)$$

$$M_{nf} = (1-\phi)M_f + \phi M_p \quad (14)$$

The first three (1, 2, 3) models used as the viscosity model in Table 2 are theoretically obtained conventional effective viscosity models and are valid for spherical particles in the micro-dimension, where there is no interaction between particles. Furthermore, the model used as the thermal conductivity model is the effective thermal conductivity model proposed by Maxwell theoretically. The other viscosity models are the correlation equations experimentally obtained by the researchers. The fourth and fifth viscosity models in Table 2 are experimental correlation equations. The fourth model was derived for nanofluid formed with 47nm Al_2O_3 nanoparticles, and the fifth model was derived for nanofluid formed with 36 nm Al_2O_3 nanoparticles and water fluid. The experimental viscosity measurement was performed by a piston-type viscometer.

Table 2. Thermal conductivity and viscosity models utilized in numerical analysis (Case 1)

Model	Researcher	Viscosity	Thermal conductivity
I	(Brinkman, 1952) [27]	$\frac{\mu_{nf}}{\mu_f} = (1-\varphi)^{-2.5}$	
II	(Einstein, 1956) [28]	$\frac{\mu_{nf}}{\mu_f} = (1+2.5\varphi)$	
III	(Batchelor, 1977) [29]	$\frac{\mu_{nf}}{\mu_f} = (1+2.5\varphi+6.5\varphi^2)$	
IV	(Nguyen, 2008) [30]	$\frac{\mu_{nf}}{\mu_f} = (1+2.5\varphi+1.5\varphi^2)$	
V	(Nguyen, 2008) [30]	$\frac{\mu_{nf}}{\mu_f} = (0.904e^{0.1483\varphi})$	$\frac{k_{nf}}{k_f} = \frac{(k_p+2k_f)-2\varphi(k_f-k_p)}{(k_p+2k_f)-\varphi(k_f-k_p)}$ (Maxwell, 1881) [8]
VI	(Chandrasekar et al., 2010) [26]	b=5300, n=2.8 $\frac{\mu_{nf}}{\mu_f} = \left(1+b\left(\frac{\varphi}{1-\varphi}\right)^n\right)$	
VII	(Maiga et al., 2004) [31]	$\frac{\mu_{nf}}{\mu_f} = (1+7.3\varphi+123\varphi^2)$	
VIII	Experimentally obtained in this study	$\frac{\mu_{nf}}{\mu_f} = (1+2.5\varphi+107.2\varphi^2)$	

Table 3. Thermal conductivity and viscosity models utilized in numerical analysis (Case 2)

Model	Researcher	Viscosity	Thermal conductivity
I	(Brinkman, 1952) [27]	$\frac{\mu_{nf}}{\mu_f} = (1-\varphi)^{-2.5}$	
II	(Einstein, 1956) [28]	$\frac{\mu_{nf}}{\mu_f} = (1+2.5\varphi)$	
III	(Batchelor, 1977) [29]	$\frac{\mu_{nf}}{\mu_f} = (1+2.5\varphi+6.5\varphi^2)$	
IV	(Nguyen, 2008) [30]	$\frac{\mu_{nf}}{\mu_f} = (1+2.5\varphi+1.5\varphi^2)$	
V	(Nguyen, 2008) [30]	$\frac{\mu_{nf}}{\mu_f} = (0.904e^{0.1483\varphi})$	$\frac{k_{nf}}{k_f}$
VI	(Chandrasekar et al., 2010) [26]	b=5300, n=2.8 $\frac{\mu_{nf}}{\mu_f} = \left(1+b\left(\frac{\varphi}{1-\varphi}\right)^n\right)$	$= \left(\frac{C_{pnf}}{C_{pf}}\right)^{-0.023}\left(\frac{\rho_{nf}}{\rho_f}\right)^{1.358}\left(\frac{M_f}{M_{nf}}\right)^{0.126}$
VII	(Maiga et al., 2004) [31]	$\frac{\mu_{nf}}{\mu_f} = (1+7.3\varphi+123\varphi^2)$	
VIII	Experimentally obtained in this study	$\frac{\mu_{nf}}{\mu_f} = (1+2.5\varphi+107.2\varphi^2)$	

When the nanoparticle size was 47 nm and the nanoparticle volumetric fraction was 1%, 4%, 9%, and 12%, the relative viscosity values were 1.12, 1.6, 3, and 5.3, respectively. When the nanoparticle size was 36 nm and the nanoparticle volumetric fraction was 2.1%, 4.3%, 8.5%, and 12.2%, the relative viscosity values were 1.1, 1.4, 2, and 3.1, respectively. As a result, it was emphasized that the dynamic viscosity of the nanofluid increased with the increased nanoparticle volumetric fraction and the results obtained from 36 nm and 47 nm were close to each other, except for the high nanoparticle volumetric fraction. Furthermore, the experimentally obtained results were compared to the Einstein and Batchelor models, and it was stated that there was an inconsistency between them. The sixth viscosity model given in Table 2 was experimentally obtained for the nanofluid prepared at different nanoparticle volumetric fractions (0.33%-5%) with 43nm Al_2O_3 nanoparticles and water base fluid. A Brookfield cone and plate viscometer were used. While it was indicated that the nanofluid viscosity increased with the nanoparticle volumetric fraction when the nanoparticle volumetric fraction was 2% at most, a nonlinear relationship was revealed between an increase in the nanofluid viscosity and nanoparticle volumetric fraction when the nanoparticle volumetric faction was more than 2%. It was argued that the reason for the formation of this situation might be more significant hydrodynamic interaction between particles when the nanoparticle volumetric fraction was more than 2%. The seventh viscosity model given in Table 2 is a model obtained by Maiga et al. [31] by the correlation of the results experimentally acquired by Wang et al. [32]. They obtained the experimental results by measuring with a viscometer for nanofluids prepared at different nanoparticle volumetric fractions (1 – 6%) with 28 nm Al_2O_3 nanoparticles and water base fluid. The experimentally obtained results were calculated with the least-squares curve, and the dynamic viscosity of the nanofluid was obtained. It was concluded that the increase in the viscosity of the Al_2O_3-water nanofluid was almost 20%-30% when the nanoparticle volumetric fraction was 3%.

The eighth viscosity model given in Table 2 is the correlation equation obtained for the nanofluid at different nanoparticle volumetric fractions (1-5%), experimentally created in this study with 80 nm Al_2O_3 nanoparticles and ethylene glycol base fluid. All rheological measurements were carried out by a stress controlled Kinexus cone and plate rheometer under constant shear rate.

The viscosity models used in Table 3 are the same as the viscosity models in Table 2, and the used thermal conductivity model is the thermal conductivity model experimentally obtained by Chandrasekar et al. (2010) [26]. The measurement of the thermal conductivity of the nanofluid was performed by a Decagon KD2 Pro device

when the volumetric fraction was 3% at most. When the nanoparticle size was 43 nm and the nanoparticle volumetric faction was 0.33%, 0.75%, 1%, 2%, and 3%, the thermal conductivity increase percentages were 1.64, 3.28, 3.43, 7.52, and 9.7, respectively. As a result, it was revealed that the thermal conductivity value of the nanofluid increased linearly with the increased nanoparticle volumetric fraction in the nanofluid, and the correlation equation was obtained. The thermal conductivities of the nanofluids prepared in the present research were measured experimentally, and the obtained correlation equation was found to be consistent with the thermal conductivity correlation equation proposed by Chandrasekar et al. (2010) [26].

3. Results and Discussion

In Tables 4 and 5, for model 1, the results obtained with four different Ra numbers (103, 104, 105, 106) were presented in the case of only heat transfer by natural convection in a square cavity geometry at five different nanoparticle volumetric fractions (1%, 2%, 3%, 4%, 5%) of the Al_2O_3 - EG nanofluid. The results were obtained for the Prandtl (Pr) number of 0.71, and u_{max} and y_{max} also, respectively, indicate the maximum value and position of the horizontal velocity component obtained along x=0.5 from the center of geometry. Similarly, v_{max} and x_{min} indicate the maximum value and position of the vertical velocity component obtained along y=0.5 from the center of the geometry. The Nu number, the measure of heat transfer, was calculated by taking the derivative of the temperature distribution along the heated wall according to component x. Nu_{max} and Nu_{min} show the maximum and minimum Nu numbers and positions computed along the hot wall. Nu_{avg} gives the average value acquired as a result of integrating the Nu number calculated along the hot wall. Nu_{avg}/Nu_{EG} shows the ratio of the average value obtained by integrating the Nu number computed along the hot wall to the calculated Nu number of the pure ethylene glycol base fluid.

Although there are many studies in the literature on nanofluids, there are few studies on the rheology of nanofluids [33-41]. In the studies conducted with nanofluids, some researchers [42, 43] argued that nanofluids behave in accordance with Newton's rule, while the others [33, 44-47] suggested that nanofluids exhibit a non-Newtonian behavior. In Figure 2, when the temperature of the Al_2O_3–EG nanofluid was 25 ^{0}C, the variation of the viscosity increase in percentage with the nanoparticle volumetric fraction was examined in different models. As can be seen from Figure 2, a considerable difference was observed in the viscosity increase of the nanofluid in the models with the increased nanoparticle volumetric fraction. For example, when the nanoparticle volumetric fraction was 5%, the viscosity increase of the nanofluid in model 6 was 140%, whereas this increase was almost 12% in model 4. The reason for this situation is the fact that the viscosity value of the nanofluid computed in the equation in model 6 was significantly higher compared to the viscosity value of the nanofluid in the equation in model 4. Furthermore, it draws attention that the viscosity increase with the increase in the nanoparticle volumetric fraction in models 5, 6, 7, and 8 was significantly higher compared to the other models. As seen from Figure 2, it is evident that the increase in the nanofluid viscosity is a function of the nanoparticle volumetric fraction. While a linear relationship was observed between the nanoparticle volumetric fraction and viscosity in models 1, 2, and 3, a nonlinear relationship was observed in the other models. The first three models are traditionally used viscosity models, and as previously mentioned, are similar to the experimental and valid data at low nanoparticle volumetric fractions. The reason for the increase in viscosity with the nanoparticle volumetric fraction, especially in models 5, 6, 7, and 8, is a result of the experimentally obtained correlation equations of these models. It is clearly observed that the viscosity increases of the experimental models are different from each other. The nanoparticles in each model and the sizes of these nanoparticles are different from each other. With the effect of the hydrodynamic force on the solid nanoparticle surface, the viscosity increases of the nanoparticles, which are accepted to be very well dispersed in the base fluid, can be affected. Since these hydrodynamic forces acting on nanoparticles of different sizes will also be different, the viscosity increase in the models may be different. For example, the viscosity increase of the nanofluid formed by Al_2O_3 with the particle size of 43 nm and water base fluid in model 6 is significantly higher in comparison with the viscosity increase of the nanofluid formed with 80 nm Al_2O_3 and ethylene glycol base fluid in model 8. Based on this, it is possible to conclude that the nanofluid viscosity increases with the decreasing nanoparticle size, similarly to the results obtained in the study by Gallego et al. (2011) [30].

For the purpose of determining the variation in the amount of heat transfer by natural convection in the square cavity geometry with the Al_2O_3-EG nanofluid, the change was given as the ratio of the average Nu number computed along the hot wall versus the nanofluid concentration to the calculated Nu number of the ethylene glycol base fluid at four different Ra numbers, 10^3, 10^4, 10^5, and 10^6, in Figure 3 (Case 1).

As is known, at low Ra numbers, heat transfer occurs with the conduction mechanism in a square cavity geometry. In Figure 3(a), upon examining the change in the average Nu number calculated along the hot wall, which is regarded as a measure of the amount of change in the heat transfer rate with the nanoparticle volumetric fraction of the Al_2O_3-EG nanofluid at low Ra numbers (Ra, 10^3), with the ratio to the calculated Nu number of the ethylene glycol base fluid, the heat transfer rate slightly decreased with the increased nanoparticle volumetric fraction in models 5, 6, 7, and 8, while the heat transfer rate increased a little bit with the

increased nanoparticle volumetric fraction in the other models. The reason why the change here was not too high was not too much variation in the heat transfer rate due to the fact that the heat transfer was realized by the conduction mechanism at Ra, 10^3, the viscosity had no impact on the heat transfer rate in this case, and the used thermal conductivity model equation was common although the viscosity equations used in the models were different. In other words, at low Ra numbers, the thermal conductivity model to be used becomes important and determines the amount of increase to be obtained from numerical analysis.

Although the heat transfer occurs by the conduction mechanism at low Ra numbers, the heat transfer is realized by the convection mechanism when the Ra number is 10^4 and higher. In this case, contrary to the case of 10^3, the viscosity models used in numerical analysis become more important. It is determined that an increase occurs in the heat transfer rate with the increased Ra number at any nanoparticle volumetric fraction at the values of the Ra number of 10^4, 10^5, and 10^6 in all models. This can be understood better from the variation of the viscosity increase with the nanoparticle volumetric fraction for different models given in Figure 3.

Figure 4 demonstrates the change in the average Nu number calculated along the hot wall versus the nanofluid concentration with the ratio to the calculated Nu number of the ethylene glycol base fluid, by considering Case 2.

The difference between the figures given here and Figure 3 (Case 1) is that the used thermal conductivity model is different. The thermal conductivity model utilized here is the correlation equation obtained from the experimental data.

Table 4. Variation of the results obtained with four different Rayleigh (Ra) numbers for model 1 with nanoparticle volumetric fraction (Ra=10^3 and 10^4)

a) Ra=10^3

Ø (%)	u_{max}	y_{max}	v_{max}	x_{min}	Nu_{max}	y_{min}	Nu_{min}	y_{max}	Nu_{avg}	Nu_{avg}/Nu_{EG}
0	3.65810344	0.81093875	3.69029864	0.81786953	1.50945640	0.99900	0.69286702	0.08123783	1.12034418	1.17369131
1	3.55160036	0.81093875	3.58008800	0.81786953	1.50021670	0.99900	0.70568006	0.08123783	1.12144911	1.13961232
2	3.44621050	0.81093875	3.47204208	0.81786953	1.49382303	0.99900	0.72039430	0.08123783	1.12451816	1.10581402
3	3.34173214	0.81093875	3.36482122	0.81786953	1.48659235	0.99900	0.73457529	0.08123783	1.12708440	1.07232775
4	3.23854643	0.81093875	3.25990584	0.81786953	1.48173333	0.99900	0.75032610	0.07687971	1.13128025	1.03920069
5	3.13630700	0.81093875	3.15496296	0.81786953	1.47357076	0.99900	0.76378893	0.07687971	1.13328362	1.00645089

b) Ra=10^4

Ø (%)	u_{max}	y_{max}	v_{max}	x_{min}	Nu_{max}	y_{min}	Nu_{min}	y_{max}	Nu_{avg}	Nu_{avg}/Nu_{EG}
0	16.29452242	0.81786953	19.75626826	0.87383996	3.69290540	0.99900	0.56798653	0.12064060	2.27853326	1
1	16.11105023	0.81786953	19.39918071	0.87383996	3.66917206	0.99900	0.57215551	0.12064060	2.26727989	0.995061134
2	15.92145724	0.81786953	19.03934156	0.87383996	3.64520741	0.99900	0.57643888	0.12064060	2.25582179	0.990032417
3	15.72580521	0.81093875	18.67647741	0.87383996	3.62036448	0.99900	0.58067215	0.12064060	2.24379426	0.984753788
4	15.52400302	0.81093875	18.31021643	0.87383996	3.59390922	0.99900	0.58465747	0.12616004	2.23077929	0.979041794
5	15.31629111	0.81093875	17.94951177	0.86818332	3.56666093	0.99900	0.58860255	0.12616004	2.21722953	0.973095091

Table 5. Variation of the results obtained with four different Rayleigh (Ra) numbers for model 1 with nanoparticle volumetric fraction (Ra=10^5 and 10^6)

c) Ra=10^5

Ø (%)	u_{max}	y_{max}	v_{max}	x_{min}	Nu_{max}	y_{min}	Nu_{min}	y_{max}	Nu_{avg}	Nu_{avg}/Nu_{EG}
0	36.74544379	0.84416170	73.78080601	0.92735897	8.54684085	0.99900	0.63786674	0.07687971	4.73379300	1
1	36.53469939	0.8441617	72.70857581	0.92735897	8.49586659	0.99900	0.64247331	0.07687971	4.71802856	0.996669808
2	36.31567196	0.8441617	71.61593655	0.92735897	8.44227153	0.99900	0.64692121	0.07687971	4.7007131	0.993011967
3	36.08907074	0.8441617	70.52711549	0.92312029	8.38646177	0.99900	0.65124959	0.07687971	4.68203683	0.98906666
4	35.85850926	0.83780294	69.44880317	0.92312029	8.32860549	0.99900	0.65543709	0.08123783	4.66193879	0.984821007
5	35.62693937	0.83780294	68.35299158	0.92312029	8.26920694	0.99900	0.65951823	0.08123783	4.64058323	0.980309707

d) Ra=10^6

Ø (%)	u_{max}	y_{max}	v_{max}	x_{min}	Nu_{max}	y_{min}	Nu_{min}	y_{max}	Nu_{avg}	Nu_{avg}/Nu_{EG}
0	84.55612499	0.889992	235.94073	0.96049229	19.759115	0.99900	0.7555784	0.0395077	9.25328477	1
		33	862		05		8	1		
1	83.93812107	0.889992	233.05367	0.95722975	19.643750	0.99900	0.7600232	0.0395077	9.23065441	0.997554343
		33	368		06		5	1		
2	83.29366501	0.889992	230.13741	0.95722975	19.522327	0.99900	0.7642888	0.0395077	9.20515637	0.994798777
		33	323		09		9	1		
3	82.62374944	0.889992	227.15080	0.95722975	19.395606	0.99900	0.7683834	0.0395077	9.17704325	0.991760599
		33	171		17		7	1		
4	81.93223668	0.884743	224.09775	0.95722975	19.263244	0.99900	0.7723086	0.0395077	9.14621627	0.988429136
		03	166		03		5	1		
5	81.24754884	0.884743	220.98254	0.95722975	19.126735	0.99900	0.7760718	0.04277025	9.1128608	0.984824423
		03	891		87		9		3	

In Figure 4(a), upon examining the change in the average Nu number calculated along the hot wall, which is evaluated as a measure of the amount of change in the heat transfer rate with the nanoparticle volumetric fraction of the Al_2O_3-EG nanofluid at low Ra numbers (Ra = 10^3) with the ratio to the calculated Nu number of the ethylene glycol base fluid, a linear increase is determined in the heat transfer rate with the increased nanoparticle volumetric fraction in all models. The difference between the increasing Ra number and models closed, and the amounts of increase converged. Similarly, to the variation in Case 1, the heat transfer rates of the models (5, 6, 7, 8) created with the experimentally obtained viscosity correlation equations are observed to decrease with the nanoparticle volumetric fraction. Furthermore, even if the thermal conductivity model changes, the change in the amount of increase and decrease does not change with the nanoparticle volumetric fraction. In this case, it becomes clear that nanofluid viscosity models are more important than nanofluid thermal conductivity models.

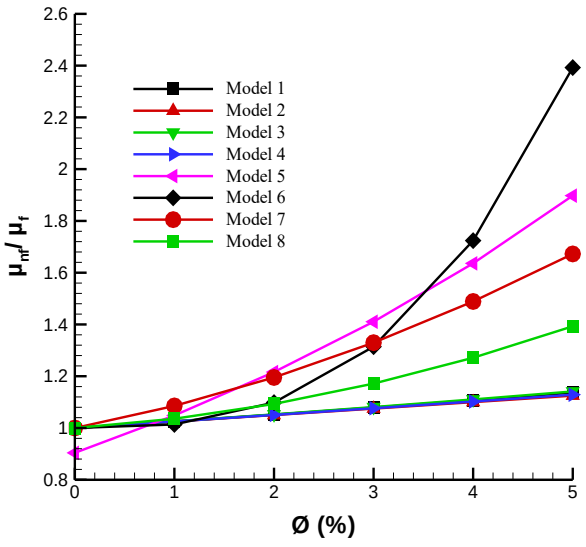

Figure 2. Variation of the relative viscosity increase with the Al_2O_3 nanoparticle volumetric fraction in percentage for different models

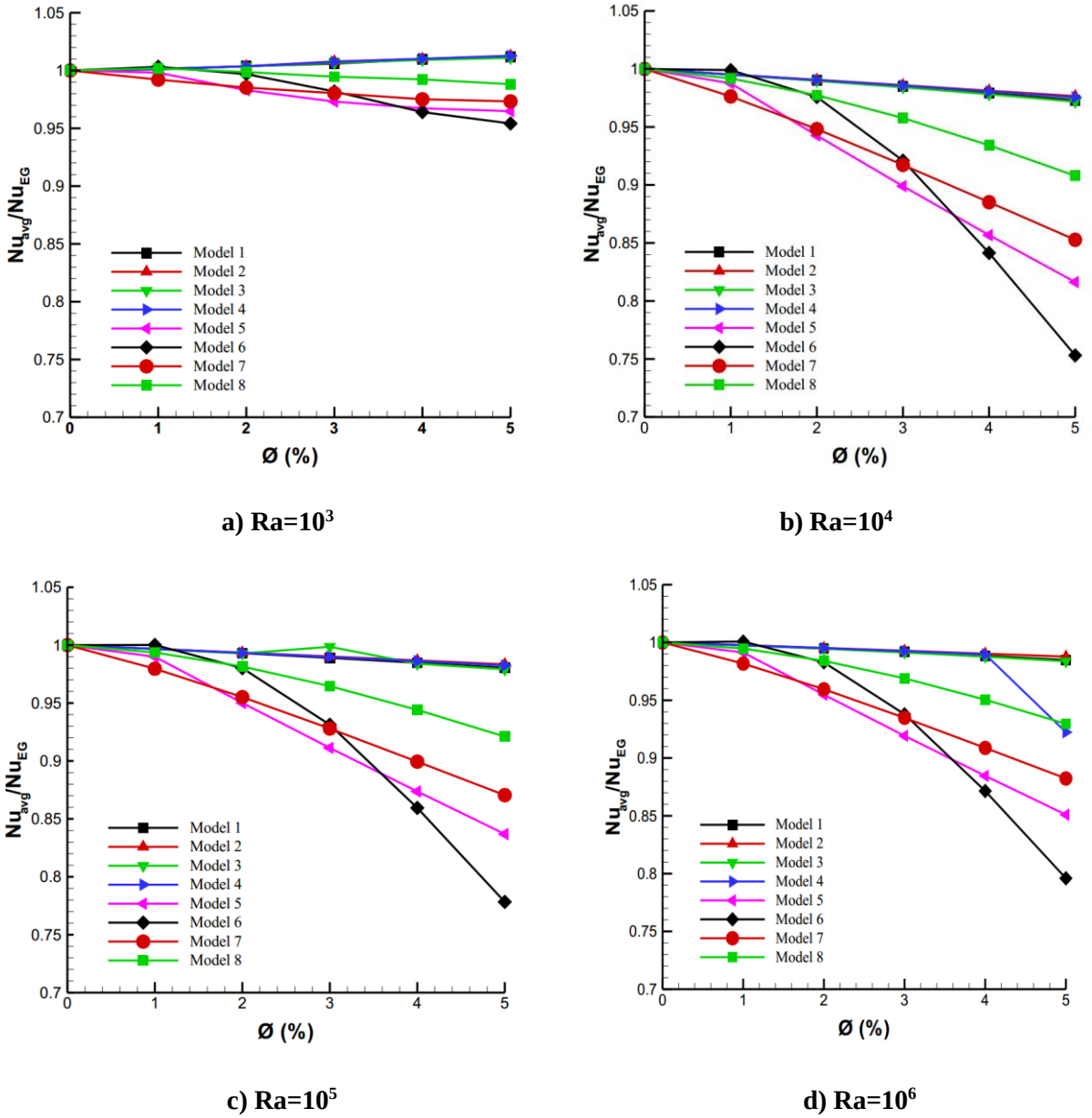

Figure 3. Variation of the ratio of the average Nu number computed along the hot wall to the Nu number calculated for pure ethylene glycol with the Al2O3 nanoparticle volumetric fraction in the square cavity geometry for different models. (Case 1)

Figures 5 and 6 demonstrate the impact of the nanoparticle volumetric fraction on the streamlines and isotherms at Ra numbers including 10^3 and 10^6 for three different models. In the figures, it is observed that only one vortex occurred in the streamlines at all Ra numbers and in all models (models 2, 6, 8). Since heat transfer by conduction is in question at a value of Ra = 10^3, the temperature contour isotherms are observed to advance almost parallel to the vertical walls. It draws attention that the structure of the vortexes formed in the center with the increased Ra number tends to be elliptical, and with the increased Ra number, the flow power efficiency increases in all models, and the boundary layer becomes more noticeable. It is revealed that the isotherms and streamlines are more severe around the hot and cold walls at a value of Ra 10^6. With the increase in the Ra number, the circulation intensity increases and, thus, the amount of heat transfer also increases. Moreover, it is observed that thermal boundary layers are generated on the walls with the same temperature with an increase in the Ra number.

The increase in the circulation intensity with the increased Ra number in the same model and at the same nanoparticle volumetric fraction can be understood from the increase in the value of in Table 6. As is seen from Table 6, the value of was found to be higher almost at all Ra numbers and all nanoparticle volumetric fractions in model 2 in comparison with models 6 and 8. In the graph of the variation of viscosity increase with the nanoparticle volumetric fraction in Figure 2, the viscosity of model 2 varies linearly with the nanoparticle volumetric fraction, whereas the viscosity of models 6 and 8 varies as the second-order polynomial

function. In other words, at the same nanoparticle volumetric fraction, the viscosity increase value obtained from models 6 and 8 is significantly higher than the viscosity increase value obtained from model 2. Accordingly, as a result of the simulation performed with model 2, there was more mixing due to low viscosity in the square cavity, and the streamline value increased due to this situation.

Figure 7 shows the streamlines and isotherms at the constant nanoparticle volumetric fraction (5%) obtained from model 8 and at Ra numbers 10^3 and 10^6. At the value of Ra=10^3, the temperature contour isotherms are observed to run almost parallel to the vertical walls. It is noteworthy that this situation changes at higher Ra numbers and the isotherms run parallel to the horizontal walls. It is observed that the structure of the vortexes formed in the center with the increase in the Ra number tends to be elliptical and the isotherms and streamlines around the hot and cold walls are more severe, especially at the value of Ra 10^6. With the increase in the Ra number, the circulation intensity increases, and, thus, the amount of heat transfer also increases. When the Ra number is 10^3 and 10^6, the values of are 0.834, and 17.810, respectively. As a result, it is found that an increase occurs in the circulation intensity with the increased Ra number.

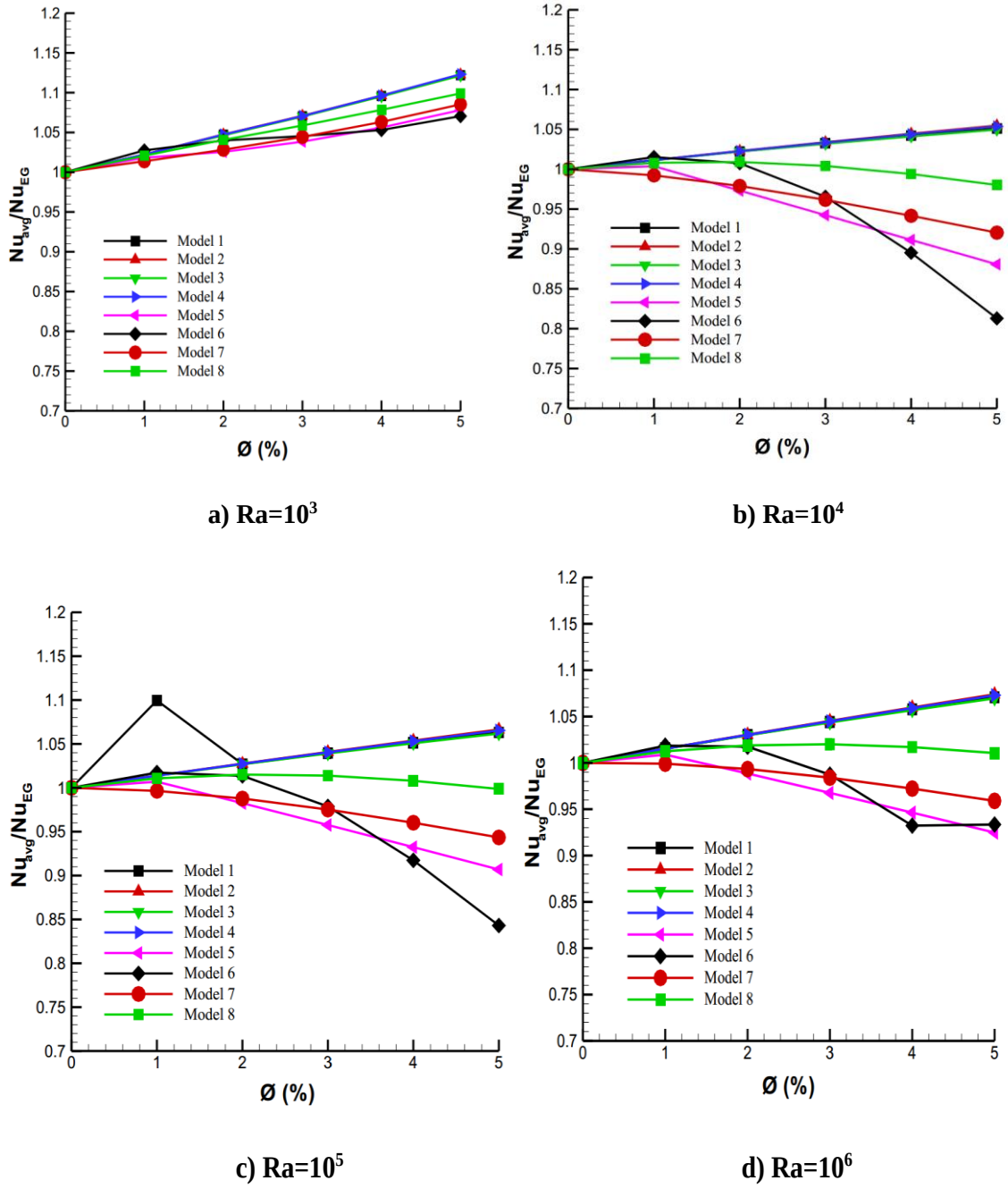

Figure 4. Variation of the ratio of the average Nu number computed along the hot wall to the Nu number calculated for pure ethylene glycol with the Al2O3 nanoparticle volumetric fraction in the square cavity geometry for different models. (Case 2)

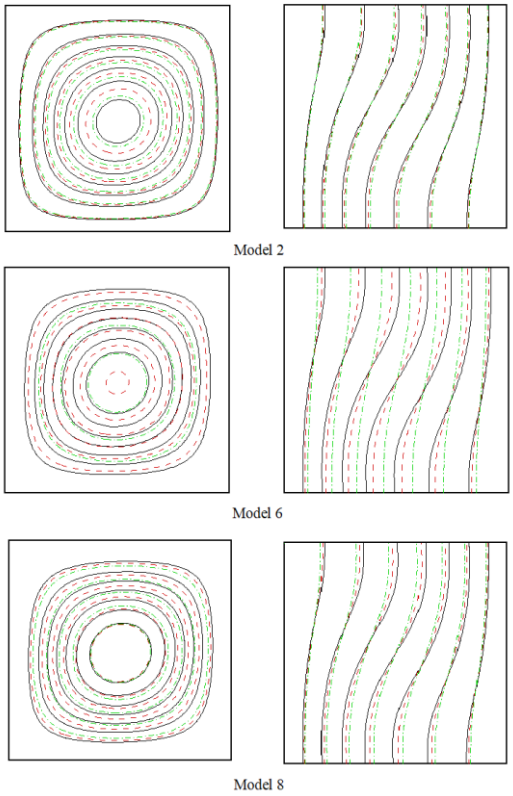

Figure 5. Streamlines (on the left) and isotherms (on the right) obtained from three various models for the Ra number of 103. Straight line: The base fluid is pure ethylene glycol; Dashed line: volumetric fraction Ø = 3%, Dot-dashed line: volumetric fraction Ø = 5%

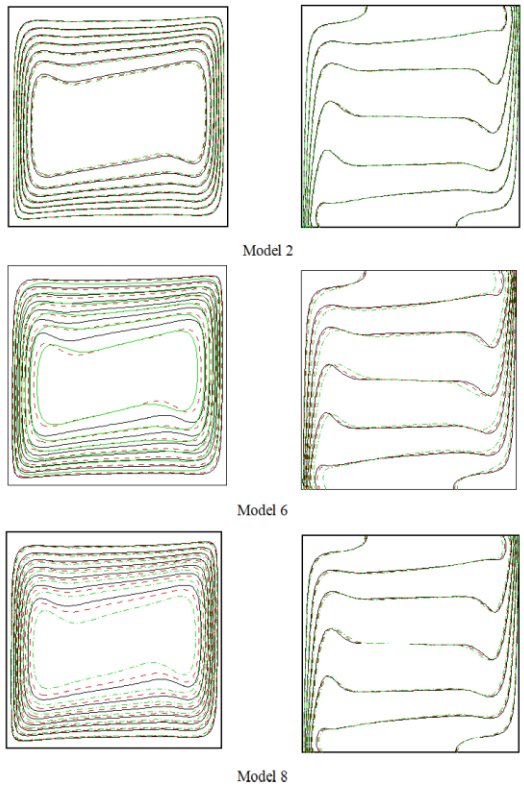

Figure 6. Streamlines (on the left) and isotherms (on the right) obtained from three various models for the Ra number of 106. Straight line: The base fluid is pure ethylene glycol; Dashed line: volumetric fraction Ø = 3%, Dot-dashed line: volumetric fraction Ø = 5%

Table 6. Variation of $|\psi_{mid}|$ values with the nanoparticle volumetric fraction and models for four different Rayleigh (Ra) numbers

	Model 2 $\lvert\psi_{mid}\rvert$	Model 6 $\lvert\psi_{mid}\rvert$	Model 8 $\lvert\psi_{mid}\rvert$
Ra = 10^3			
Ø = 0	1.17369131	1.17369131	1.17369131
Ø = 3	1.07601917	0.89604768	0.99567184
Ø = 5	1.01605693	0.49698172	0.8343271
Ra = 10^4			
Ø = 0	5.17565661	5.17565661	5.17565661
Ø = 3	5.01141879	4.55546043	4.81458625
Ø = 5	4.90059342	3.28177697	4.41558277
Ra = 10^5			
Ø = 0	10.87485547	10.87485547	10.87485547
Ø = 3	10.78205462	10.22409723	10.54075466
Ø = 5	10.71546039	8.70841675	10.12306774
Ra = 10^6			
Ø = 0	18.79429992	18.79429992	18.79429992
Ø = 3	18.72688246	17.91086387	18.3730733
Ø = 5	18.67433262	15.76604599	17.81044532

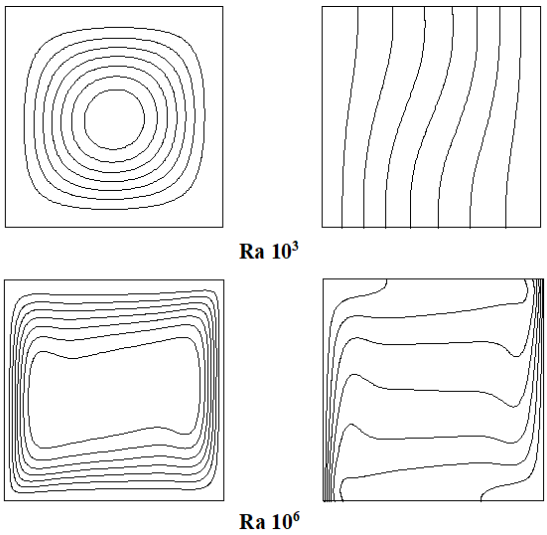

Figure 7. Streamlines (on the left) and isotherms (on the right) at the Ra number of 10^3 and 10^6 obtained from model 8 for the nanoparticle volumetric fraction of 5%

4. Conclusions

In this study, the numerical analysis of natural convection heat transfer in cavity that had two dimensions was performed. As a medium for heat transfer, Al_2O_3-EG nanofluid and incompressible Newtonian fluid were utilized.

With the aim of solving governing equations that have two dimensions, a non-uniform four-point fourth-order scheme was used and applied by utilizing the finite volume method. The systematical analysis of natural convection heat transfer was conducted for different Rayleigh numbers, different models for different concentrations of nanoparticles for the nanofluid case. The conclusions presented below were obtained based on the numerical tests:

- At low Ra numbers, a very slight increase was observed in the heat transfer rate with the increased nanoparticle fraction in models 1, 2, and 3, whereas a very slight decrease was observed in the other models. In this case, the change was not too much because the thermal conductivity equation was more significant than the viscosity equations at low Ra numbers and the thermal conductivity equation used in the models was common. In other words, the thermal conductivity model to be used at low Ra numbers gains importance and determines the result to be obtained from numerical analysis.
- Since heat transfer is conducted by the convection mechanism at high Ra numbers, in this case, the viscosity will increase with the increased nanoparticle volumetric fraction, and, thus, the fluid's mobility will decrease, and the heat transfer rate will also decrease. A decrease was observed in the heat transfer rate with the increased nanoparticle volumetric fraction in all of the experimental correlation models (5, 6, 7, 8), and, as a result, the viscosity models gained importance at high Ra numbers.
- It was revealed that an increase occurred in the heat transfer rate with the increasing Ra number at the fixed nanoparticle volumetric fraction.
- In Case 2, the heat transfer rate was found to be higher in all models in comparison with Case 1 at the constant nanoparticle volumetric fraction and constant Ra number, and the fit between the models was observed to be better in comparison with Case 1.
- Since the change trends of the models with the increased nanoparticle volumetric fraction were almost the same at high Ra numbers in Case 1 and Case 2, it was revealed that the used viscosity model was superior to the thermal conductivity model.

Declaration

The authors declared no potential conflicts of interest with respect to the research, authorship, and/or publication of this article. The authors also declared that this article is original, was prepared in accordance with international publication and research ethics, and ethical committee permission or any special permission is not required.

Author Contributions

N. Keklikcioglu Cakmak developed the methodology, and planned the study. N. Keklikcioglu Cakmak wrote the manuscript. K. Yapici and H. H. Durmazucar participated analysis and made proofreading of manuscript.

Acknowledgment

This study supported by The Scientific Research Project Fund of Sivas Cumhuriyet University under Research Project (project number: M-489).

References

1. Baïri, A., E. Zarco-Pernia, and J.-M.G. De María, *A review on natural convection in enclosures for engineering applications. The particular case of the parallelogrammic diode cavity.* Applied Thermal Engineering, 2014. **63**(1): p. 304-322.
2. Tyagi, H., P. Phelan, and R. Prasher, *Predicted efficiency of a low-temperature nanofluid-based direct absorption solar collector.* Journal of solar energy engineering, 2009. **131**(4).
3. Mahian, O., et al., *A review of the applications of nanofluids in solar energy.* International Journal of Heat and Mass Transfer, 2013. **57**(2): p. 582-594.
4. Tyagi, H., *Radiative and combustion properties of nanoparticle-laden liquids*. 2008: Arizona State University.
5. Çakmak, N.K., *Experımental study of thermal conductıvıty of borıc acıd-water solutıons.* 2019. **50**(17): p. 1675-1684.
6. Hussein, A.K., et al., *The effect of the baffle length on the natural convection in an enclosure filled with different nanofluids.* Journal of Thermal Analysis and Calorimetry, 2020.
7. Said, Z., et al., *Recent advances on nanofluids for low to medium temperature solar collectors: energy, exergy, economic analysis and environmental impact.* Progress in Energy and Combustion Science, 2021. **84**: p. 100898.
8. Maxwell, J.C., *A treatise on electricity and magnetism, Clarendon.* Oxford, 1881. **314**: p. 1873.
9. Choi, S.U. and J.A. Eastman, *Enhancing thermal conductivity of fluids with nanoparticles*. 1995, Argonne National Lab., IL (United States).
10. Bazdar, H., et al., *Numerical investigation of turbulent flow and heat transfer of nanofluid inside a wavy microchannel with different wavelengths.* Journal of Thermal Analysis and Calorimetry, 2020. **139**(3): p. 2365-2380.
11. Keklikcioglu, O., T. Dagdevir, and V. Ozceyhan, *Heat transfer and pressure drop investigation of graphene nanoplatelet-water and titanium dioxide-water nanofluids in a horizontal tube.* Applied Thermal Engineering, 2019. **162**: p. 114256.
12. Khanafer, K., K. Vafai, and M. Lightstone, *Buoyancy-driven heat transfer enhancement in a two-dimensional enclosure utilizing nanofluids.* International journal of heat and mass transfer, 2003. **46**(19): p. 3639-3653.
13. Hwang, K.S., J.-H. Lee, and S.P. Jang, *Buoyancy-driven heat transfer of water-based Al2O3 nanofluids in a rectangular cavity.* International Journal of Heat and Mass Transfer, 2007. **50**(19-20): p. 4003-4010.
14. Abu-Nada, E., *Effects of variable viscosity and thermal conductivity of Al2O3–water nanofluid on heat transfer enhancement in natural convection.* International Journal of Heat and Fluid Flow, 2009. **30**(4): p. 679-690.
15. Oztop, H.F. and E. Abu-Nada, *Numerical study of natural convection in partially heated rectangular enclosures filled*

with nanofluids. International journal of heat and fluid flow, 2008. **29**(5): p. 1326-1336.

16. Corcione, M., M. Cianfrini, and A. Quintino, *Enhanced natural convection heat transfer of nanofluids in enclosures with two adjacent walls heated and the two opposite walls cooled.* International Journal of Heat and Mass Transfer, 2015. **88**: p. 902-913.
17. Mahalakshmi, T., et al., *Natural convective heat transfer of Ag-water nanofluid flow inside enclosure with center heater and bottom heat source.* Chinese Journal of Physics, 2018. **56**(4): p. 1497-1507.
18. Yıldız, Ç., M. Arıcı, and H. Karabay, *Comparison of a theoretical and experimental thermal conductivity model on the heat transfer performance of Al2O3-SiO2/water hybrid-nanofluid.* International Journal of Heat and Mass Transfer, 2019. **140**: p. 598-605.
19. Wen, D. and Y. Ding, *Formulation of nanofluids for natural convective heat transfer applications.* International Journal of Heat and Fluid Flow, 2005. **26**(6): p. 855-864.
20. Ho, C., et al., *Natural convection heat transfer of alumina-water nanofluid in vertical square enclosures: an experimental study.* International Journal of Thermal Sciences, 2010. **49**(8): p. 1345-1353.
21. Keklikcioğlu Çakmak, N., Durmazuçar, H , Yapıcı, K . *A numerical study of mixed convection heat transfer in a lid-driven cavity using Al2O3-water nanofluid* . International Journal of Chemistry and Technology, 2020. **4**(1): p. 22-37.
22. Putra, N., W. Roetzel, and S.K. Das, *Natural convection of nano-fluids.* Heat and mass transfer, 2003. **39**(8-9): p. 775-784.
23. Abu-Nada, E., Z. Masoud, and A. Hijazi, *Natural convection heat transfer enhancement in horizontal concentric annuli using nanofluids.* International Communications in Heat and Mass Transfer, 2008. **35**(5): p. 657-665.
24. Kim, C.S., K. Okuyama, and J.F. de la Mora, *Performance evaluation of an improved particle size magnifier (PSM) for single nanoparticle detection.* Aerosol Science & Technology, 2003. **37**(10): p. 791-803.
25. Yapici, K. and S. Obut, *Benchmark results for natural and mixed convection heat transfer in a cavity.* International Journal of Numerical Methods for Heat & Fluid Flow, 2015.
26. Chandrasekar, M., S. Suresh, and A.C. Bose, *Experimental investigations and theoretical determination of thermal conductivity and viscosity of Al2O3/water nanofluid.* Experimental Thermal and Fluid Science, 2010. **34**(2): p. 210-216.
27. Brinkman, H., *The viscosity of concentrated suspensions and solutions.* The Journal of Chemical Physics, 1952. **20**(4): p. 571-571.
28. Einstein, A., *Investigations on the Theory of the Brownian Movement*. 1956: Courier Corporation.
29. Batchelor, G., *The effect of Brownian motion on the bulk stress in a suspension of spherical particles.* Journal of fluid mechanics, 1977. **83**(1): p. 97-117.
30. Nguyen, C., et al., *Viscosity data for Al2O3–water nanofluid—hysteresis: is heat transfer enhancement using nanofluids reliable?* International journal of thermal sciences, 2008. **47**(2): p. 103-111.
31. Maïga, S.E.B., et al., *Heat transfer behaviours of nanofluids in a uniformly heated tube.* Superlattices and Microstructures, 2004. **35**(3-6): p. 543-557.
32. Wang, X., X. Xu, and S.U. Choi, *Thermal conductivity of nanoparticle-fluid mixture.* Journal of thermophysics and heat transfer, 1999. **13**(4): p. 474-480.
33. Ding, Y., et al., *Heat transfer of aqueous suspensions of carbon nanotubes (CNT nanofluids).* International Journal of Heat and Mass Transfer, 2006. **49**(1-2): p. 240-250.
34. Yapici, K., et al., *Rheological characterization of polyethylene glycol based TiO 2 nanofluids.* Korea-Australia Rheology Journal, 2014. **26**(4): p. 355-363.
35. Wang, L., H. Chen, and S. Witharana, *Rheology of nanofluids: a review.* Recent patents on nanotechnology, 2013. **7**(3): p. 232-246.
36. Sharma, A.K., A.K. Tiwari, and A.R. Dixit, *Rheological behaviour of nanofluids: a review.* Renewable and Sustainable Energy Reviews, 2016. **53**: p. 779-791.
37. Tiwari, A.K., et al., *4S consideration (synthesis, sonication, surfactant, stability) for the thermal conductivity of CeO2 with MWCNT and water based hybrid nanofluid: An experimental assessment.* Colloids and Surfaces A: Physicochemical and Engineering Aspects, 2021. **610**: p. 125918.
38. Tiwari, A.K., et al., *3S (Sonication, surfactant, stability) impact on the viscosity of hybrid nanofluid with different base fluids: An experimental study.* Journal of Molecular Liquids, 2021. **329**: p. 115455.
39. Keklikcioglu Cakmak, N., *The impact of surfactants on the stability and thermal conductivity of graphene oxide de-ionized water nanofluids.* Journal of Thermal Analysis and Calorimetry, 2020. **139**(3): p. 1895-1902.
40. Keklikcioğlu Çakmak, N., Temel, Ü , Yapıcı, K, *Examination of Rheological Behavior of Water-Based Graphene Oxide Nanofluids* Cumhuriyet Science Journal, 2017. **38**(4): p. 176-183.
41. Cakmak, N.K., et al., *Preparation, characterization, stability, and thermal conductivity of rGO-Fe3O4-TiO2 hybrid nanofluid: An experimental study.* Powder Technology, 2020. **372**: p. 235-245.
42. Das, S.K., N. Putra, and W. Roetzel, *Pool boiling characteristics of nano-fluids.* International journal of heat and mass transfer, 2003. **46**(5): p. 851-862.
43. Prasher, R., et al., *Measurements of nanofluid viscosity and its implications for thermal applications.* Applied physics letters, 2006. **89**(13): p. 133108.
44. He, Y., et al., *Heat transfer and flow behaviour of aqueous suspensions of TiO2 nanoparticles (nanofluids) flowing upward through a vertical pipe.* International journal of heat and mass transfer, 2007. **50**(11-12): p. 2272-2281.
45. Kwak, K. and C. Kim, *Viscosity and thermal conductivity of copper oxide nanofluid dispersed in ethylene glycol.* Korea-Australia Rheology Journal, 2005. **17**(2): p. 35-40.
46. Studart, A.R., et al., *Rheology of concentrated suspensions containing weakly attractive alumina nanoparticles.* Journal of the American Ceramic Society, 2006. **89**(8): p. 2418-2425.
47. Tseng, W.J. and K.-C. Lin, *Rheology and colloidal structure of aqueous TiO2 nanoparticle suspensions.* Materials science and engineering: A, 2003. **355**(1-2): p. 186-192.